

## IN THE LARGE ASPECT RATIO FULL TUNGSTEN TOKAMAK WEST

J. Gaspar<sup>a</sup>, Y. Corre<sup>b</sup>, C. Bourdelle<sup>b</sup>, S. Brezinsek<sup>c</sup>, J. Bucalossi<sup>b</sup>, N. Chanet<sup>b</sup>, R. Dejarnac<sup>d</sup>, N. Fedorczak<sup>b</sup>, M. Firdaouss<sup>b</sup>, J.-L. Gardarein<sup>a</sup>, J. P. Gunn<sup>b</sup>, G. Laffont<sup>e</sup>, T. Loarer<sup>b</sup>, C. Pocheau<sup>b</sup>, E. Tsiatronis<sup>b</sup> and the WEST team\*

<sup>a</sup> Aix Marseille Univ, CNRS, IUSTI, Marseille, France / <sup>b</sup> CEA, Institute for Research on Fusion by Magnetic confinement, 13108 Saint-Paul-Lez-Durance, France /

<sup>c</sup> FZ Jülich, Institut für Energie - und Klimaforschung - Plasmaphysik, TEC, 52425 Jülich, Germany / <sup>d</sup> Institute of Plasma Physics, Czech Academy of Sciences, Prague, Czech Republic / <sup>e</sup> CEA, LIST, Gif-sur-Yvette Cedex 91191, France / \* See <http://west.cea.fr/WESTteam>

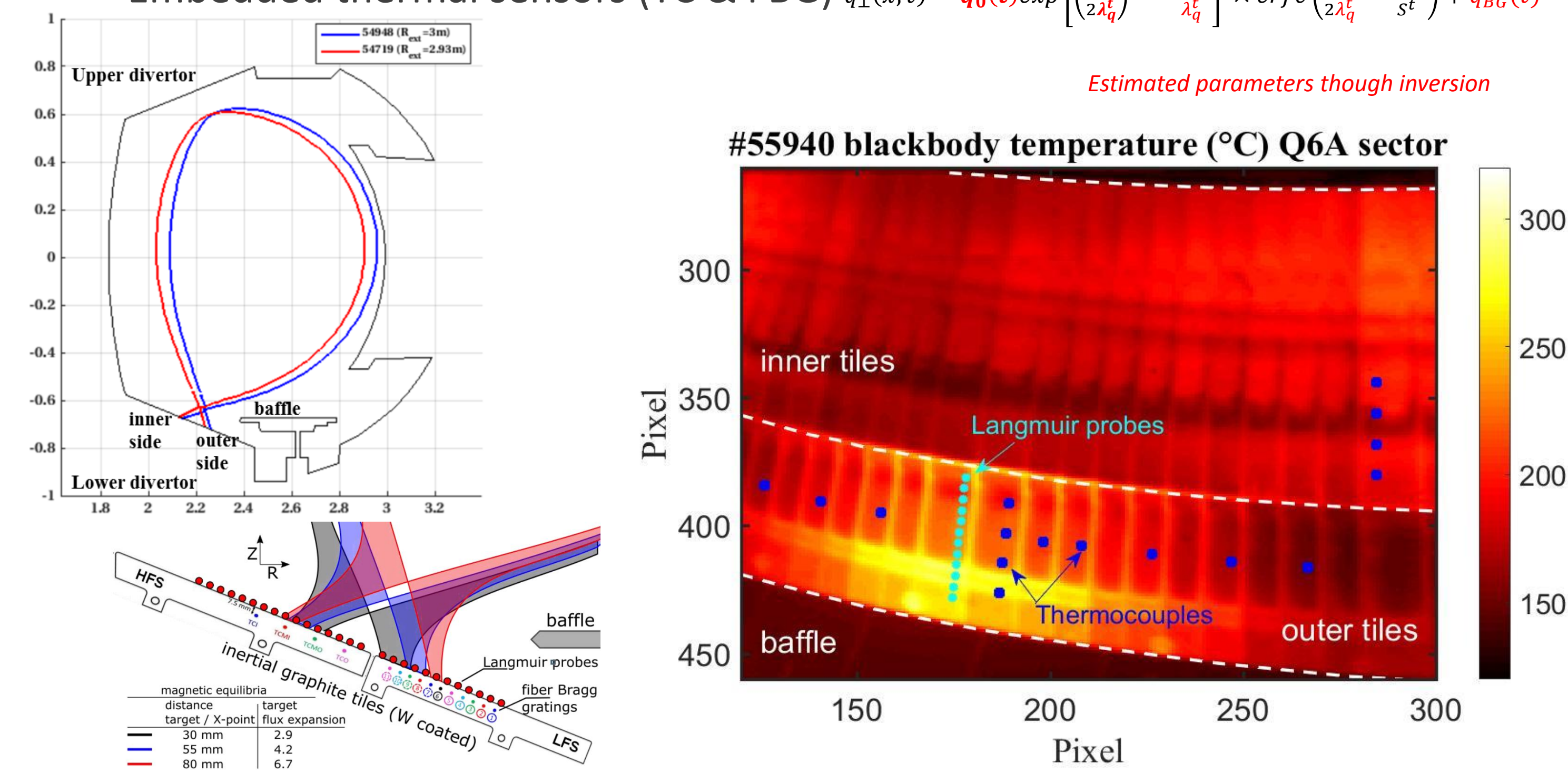
### ABSTRACT

• A large database including different magnetic equilibrium and input power is investigated to compare the heat load pattern (location, amplitude of the peak and heat flux decay length) on the inner and outer regions as function of the continuous progress achieved in WEST : from the first ohmic diverted plasma (obtained during the second experimental campaign C2 in 2018) up to the high power (up to 8 MW total injected) and high energy (up to 90 MJ injected energy in lower single null configuration) steady state experiments performed in the last experimental campaign (C4 in 2019).

### Diagnostic set-up

WEST: full metallic tokamak + extensive set of diagnostics for heat load measurement on lower divertor W tiles (W coated uncooled graphite tiles):

- Flush mounted Langmuir probes (LP)  $q_{||} = \gamma j_{SAT} T_e$  with  $\gamma \approx 7$
- Infra-red (IR) thermography  $q_{\perp}$  estimated with TEDDY code
- Embedded thermal sensors (TC & FBG)  $q_{\perp}(x, t) = q_0(t) \exp\left(\frac{s^2}{2\lambda_q^t} - \frac{s-s_0}{\lambda_q^t}\right) \times \text{erfc}\left(\frac{s}{2\lambda_q^t} - \frac{s-s_0}{s^t}\right) + q_{BG}(t)$



### Heat flux comparison FBG/TC/LP/IR

#### Database

165 L-mode Lower Single Null (LSN) discharges with  $P_{tot}$  from 1 to 8 MW  $B_T \approx 3.7$  T and  $I_p$  from 300 to 700 kA (corresponding  $q_{95}$  from 3.2 to 7.8)

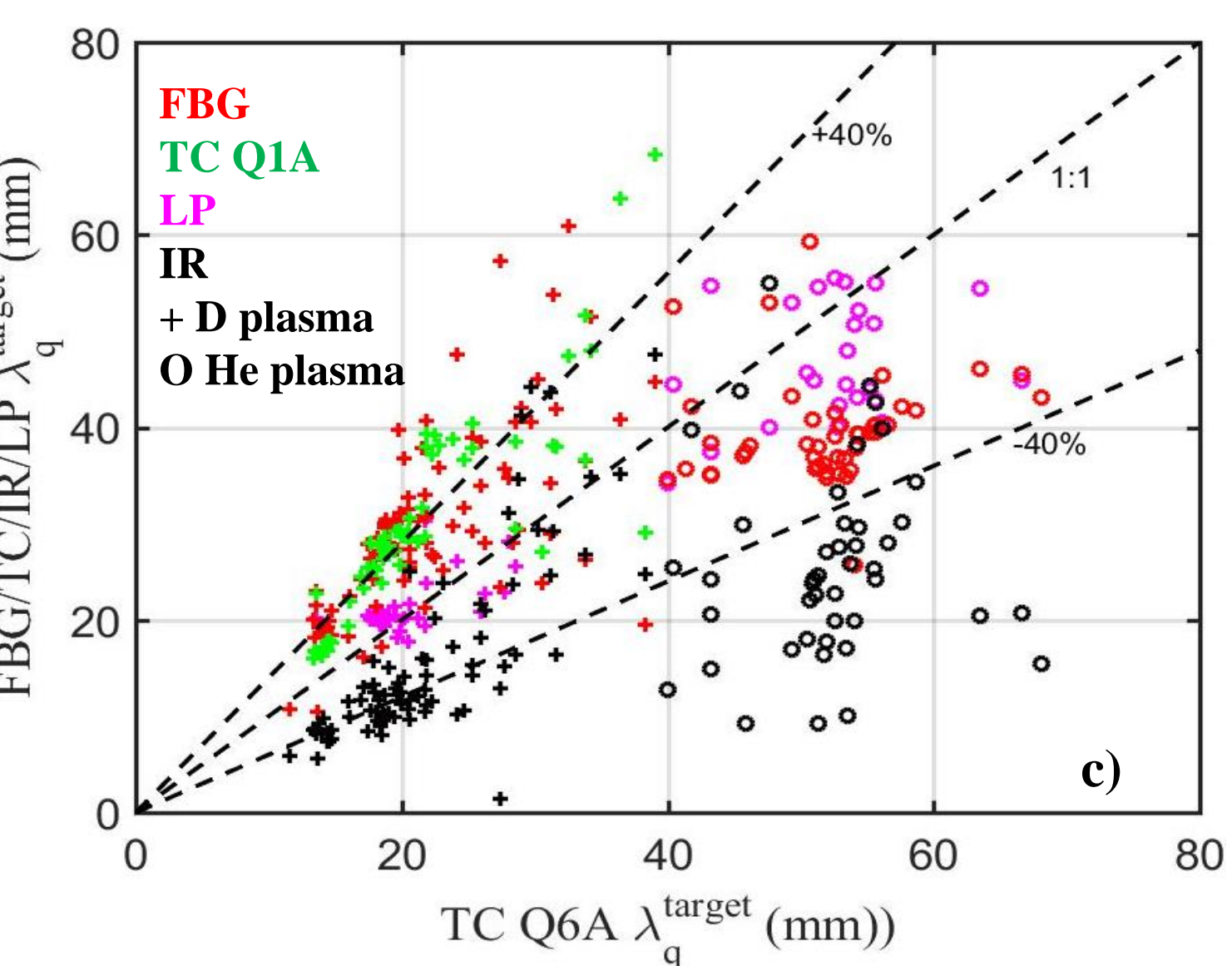
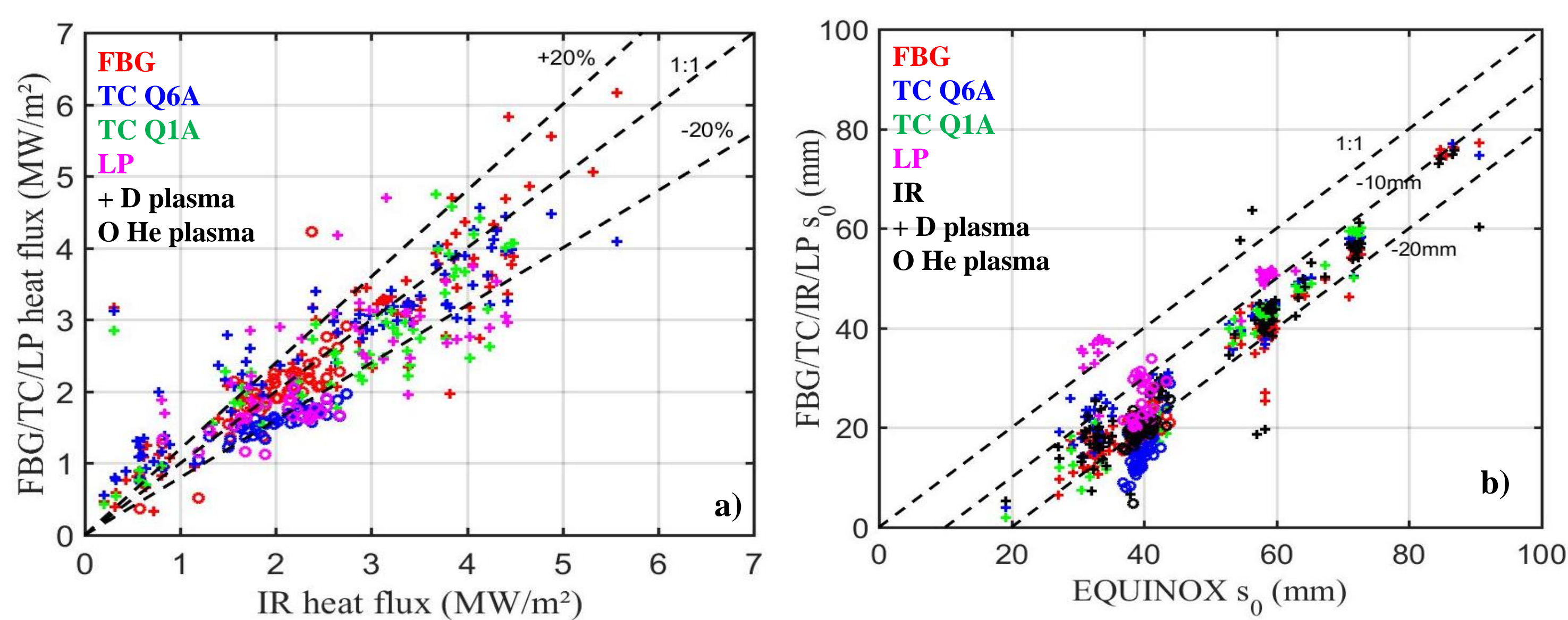


Fig b): Inward shift from 1 to 2 cm between the diagnostics and the magnetic reconstruction.

Fig c): 3 groups of  $\lambda_q^t$  appears:

- TC<sub>Q6A</sub> & LP (Q6A) (consecutive PFCs) [middle]
- IR (same PFC as TC<sub>Q6A</sub>) [-40%]
- FBG (Q3A) & TC<sub>Q1A</sub> [+40%] (180° and 60° toroidally spaced with other diag)

#### Crosscheck

IR inversion and LP measurement fitted with Eich formula (see above) with averaged data over 1s to extract  $q_{peak}$ ,  $\lambda_q^t$  and  $s_0$  for comparison to TC/FBG

Fig a): good agreement for  $q_{peak}$  with all diagnostics in the range  $\pm 20\%$

### Divertor heat load steady progress during WEST phase 1

Divertor heat flux increase over the campaigns from about 0.2 MW/m<sup>2</sup> with 2.3 MW of Low Hybrid Current Drive (LHCD) during C2 to 6 MW/m<sup>2</sup> with 4MW of LHCD during C4 (Fig d)) → 10MW/m<sup>2</sup> can be reached with ≈7MW of RF heating in L-mode. The ≈1.7 increase from C3 to C4 is observed for all pulses on outer and inner side (Fig d)), despite equivalent plasma parameters ( $I_p$ , density, magnetic field) and estimated  $\lambda_q^t$  (Fig e)).

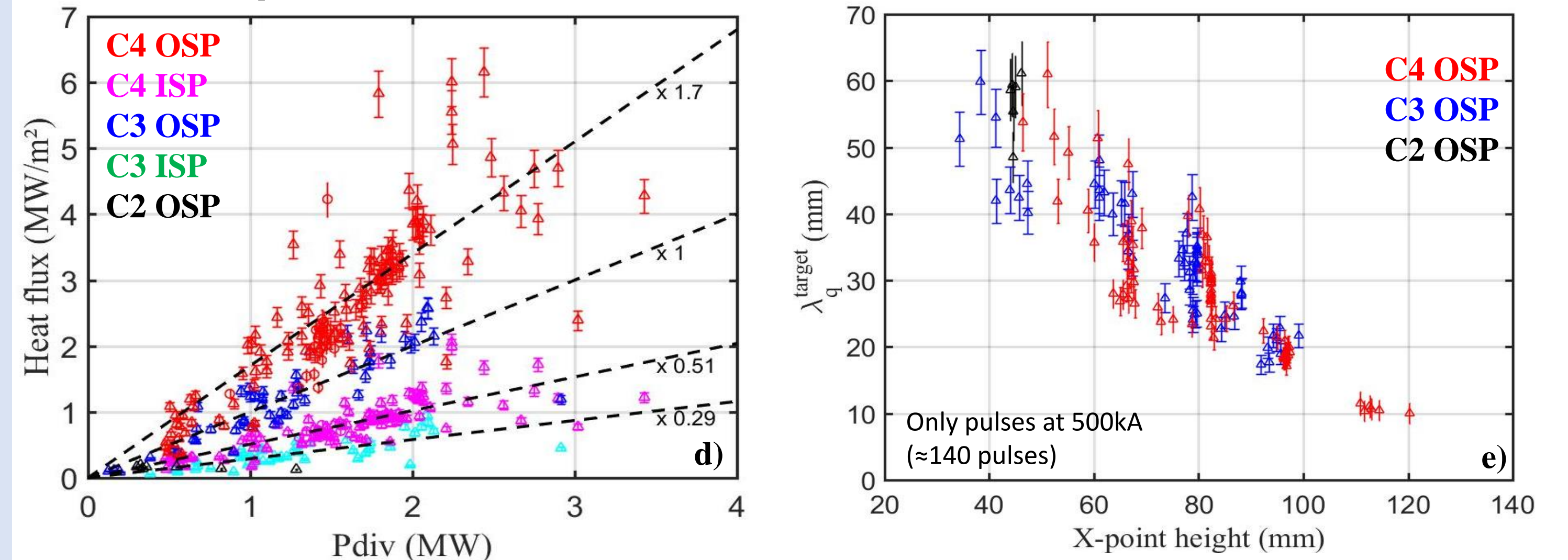


Fig f) and g): The divertor heat load increase is also observed with the increase of the absorbed energy for 1272 pulses of the different campaigns (E calculated from the cooling phase of the inertial PFC).

Same trend for C3 & C4 for the absorbed energy versus  $E_{inj}$  in USN → equivalent radiated and neutral loads in USN

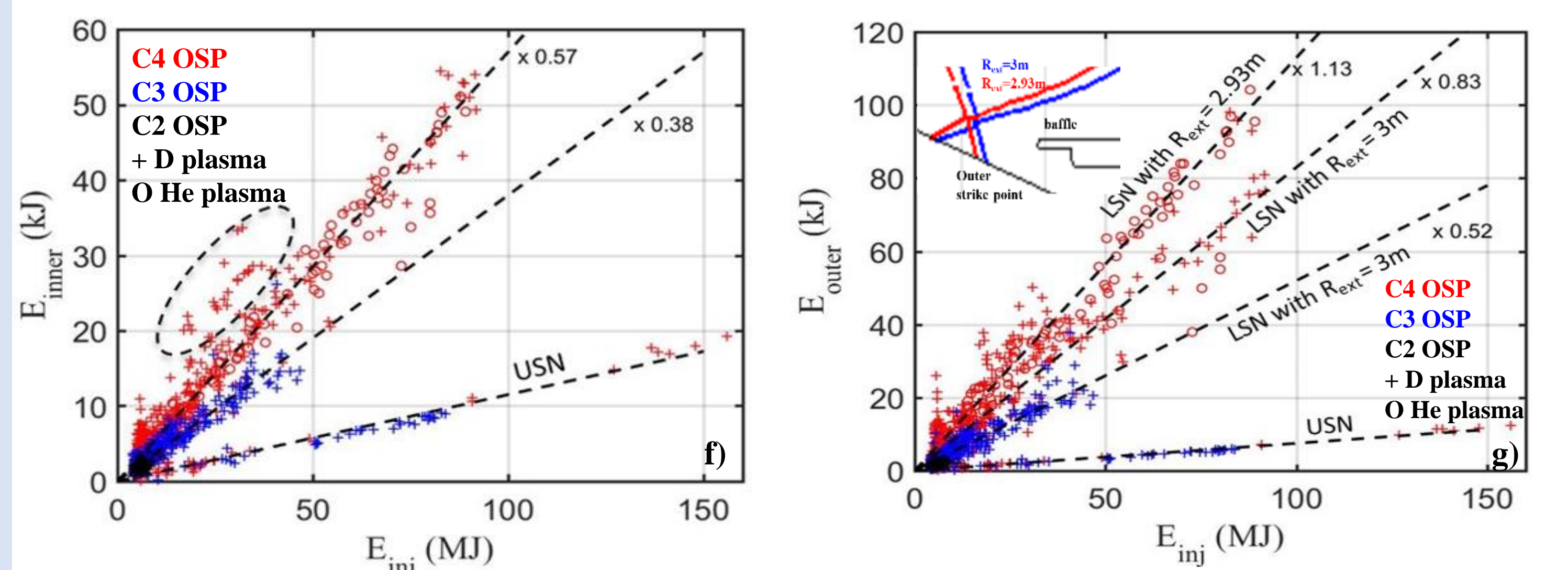
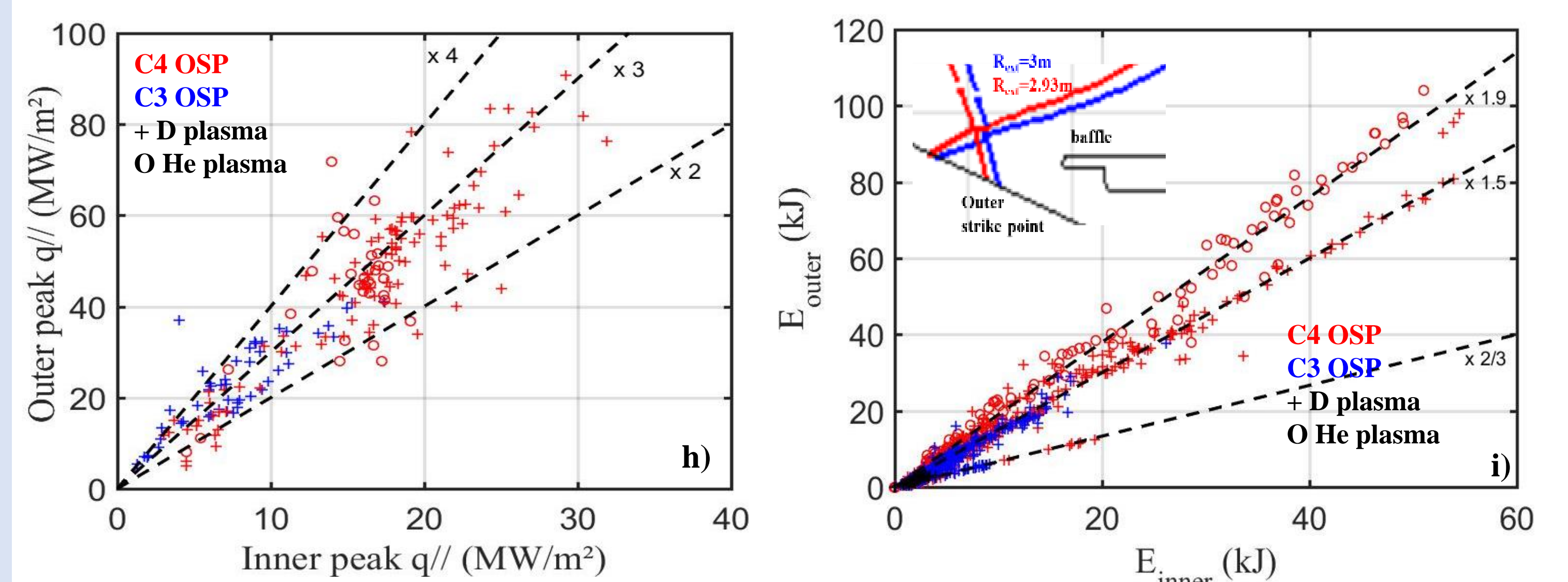


Fig h): Peak  $q_{||}$  asymmetry about 3 (3/4 1/4) and equivalent for the whole database no dependency found with  $P_{div}$ , density or  $q_{95}$  but pulses mainly at 500kA and 300kA with small density variation at same  $I_p$ .

Fig i):  $E_{outer}/E_{inner}$  equivalent for the campaigns but affected by the baffle screening



### CONCLUSION

- $q_{peak}$  from the whole set of diagnostics is in good agreement in the  $\pm 20\%$  range
- $\lambda_q^t$  and  $s_0$  scale quite linearly with the X-point height as expected
- But  $\lambda_q^t$  shows significant discrepancy between diagnostics and location in the machine ( $\pm 40\%$  range). → improve IR processing ( $\epsilon(s, T)$ ) and post-mortem analysis TC/FBG
- $q_{peak}$  has followed the continuous progress achieved in WEST and increase over the campaigns from 0.2MW/m<sup>2</sup> to 6MW/m<sup>2</sup> → 10 MW/m<sup>2</sup> steady state accessible with ≈ 7 MW of additional power in L-mode discharge
- Heat load distribution is clearly asymmetric with a 3/4 and 1/4 distribution for  $q_{||}$  higher on the outer region as commonly observed in forward-B configuration

### ACKNOWLEDGEMENTS

• This work has been carried out thanks to the support of the A\*MIDEX project (n° ANR-11-IDEX-0001-02) funded by the "Investissements d'Avenir" French Government program, managed by the French National Research Agency (ANR).

• This work has been carried out within the framework of the EUROfusion Consortium and has received funding from the Euratom research and training programme 2014-2018 and 2019-2020 under grant agreement No 633053. The views and opinions expressed herein do not necessarily reflect those of the European Commission.